Original

ISSN 0946-1965

DOI 10.5414/CP204217
e-pub: ●●month ●●day, ●●year

Novel intranasal treatment for anxiety disorders using amiloride, an acid-sensing ion channel antagonist: Pharmacokinetic modeling and simulation

Mahmoud Azzeh[1], Marco Battaglia[2,3], Simon Davies[2], John Strauss[2,3], Prashant Dogra[4,5], and Venkata Yellepeddi[6,7]

[1]College of Medicine, Mohammed Bin Rashid University, Dubai, UAE, [2]Centre for Addiction and Mental Health, [3]Department of Psychiatry, University of Toronto, Toronto, ON, Canada, [4]Mathematics in Medicine Program, Houston Methodist Research Institute, Houston, TX, [5]Department of Physiology and Biophysics, Weill Cornell Medical College, New York, NY, [6]Division of Clinical Pharmacology, Department of Pediatrics, School of Medicine, and [7]Department of Pharmaceutics and Pharmaceutical Chemistry, College of Pharmacy, University of Utah, Salt Lake City, UT, USA

Key words
acid-sensing ion channels – anxiety – physiologically-based pharmacokinetic modeling – amiloride – nasal spray – permeability – blood-brain barrier – area under the curve

Abstract. Objective: To develop a physiologically based pharmacokinetic (PBPK) model for amiloride, an acid-sensing ion channel (ASIC) antagonist, and to simulate its pharmacokinetics in plasma and the central nervous system following intranasal administration in a virtual human population. Materials and methods: We first developed a PBPK model of amiloride after oral administration and optimized the model using data from 5 clinical studies. Next, we added a nasal compartment to the amiloride oral PBPK model and parameterized using data from previous clinical studies. We simulated amiloride's pharmacokinetics in plasma, brain, and cerebrospinal fluid (CSF) after intranasal administration of amiloride at various doses in a virtual human population. Results: The target amiloride concentration in the central nervous system required for maximal ASIC inhibition was achieved with a 75-mg intranasal amiloride dose. However, this finding is based on simulations performed using a mathematical model and needs to be further validated with appropriate clinical data. Conclusion: The nasal PBPK model of amiloride could be used to design future clinical studies and allow for successful clinical translation of intranasal amiloride formulation.

What is known about the subject

- Anxiety disorders are the most common mental health conditions, and there is a significant unmet need to develop new therapeutics to treat anxiety disorders.
- Amiloride, an ASIC antagonist, has shown pre-clinical efficacy potential in reducing anxiety and can potentially be translated for clinical use in humans.
- Amiloride can be formulated and administered as a nasal spray and can result in rapid onset of action and improved absorption into brain tissue.

Supplemental material is available without charge at: www.clinpharmacol.com Vol. ●●●, issue ●●●.

Azzeh M, Battaglia M, Davies S, Strauss J, Dogra P, Yellepeddi V. Novel intranasal treatment for anxiety disorders using amiloride, an acid-sensing ion channel antagonist: Pharmacokinetic modeling and simulation. Int J Clin Pharmacol Ther. ●●●; ●●●: ●●●-11. DOI 10.5414/CP204217
citation

Received December 27, 2021; accepted January 31, 2022
DOI 10.5414/CP204217, PMID: ●●●, e-pub: ●●month ●●day, ●●year

Correspondence to: Venkata Yellepeddi, ●●● **MD,…?**, Division of Clinical Pharmacology, Department of Pediatrics, School of Medicine, University of Utah, 1279 E Quail Grove Circle, Salt Lake City, UT 84121, USA, **venkata.yellepeddi@hsc.utah.edu**

What this study adds

- This is the first study to show that the pharmacokinetics of intranasal amiloride can be simulated in a virtual human population using a PBPK model.
- The simulations from PBPK modeling showed that amiloride reaches the brain rapidly when compared to other routes of administration.
- The simulations also showed that intranasal administration of amiloride at 75-mg dose will result in maximum concentrations in the brain ASIC inhibition activity. However, further studies are required to generate data to verify and validate the data simulated by the current PBPK model.

Introduction

Anxiety disorders are the most prevalent mental health conditions, with up to 34% of the general population diagnosed with at least one anxiety disorder in their lifetime [1, 2]. Anxiety disorders also account for the largest cost fraction (32%) of all mental disorders [3]. A subset of anxiety disorders is panic disorder, which is characterized by recurrent unexpected panic attacks [4]. The standard first-line pharmacological treatments for panic disorder are selective serotonin reuptake inhibitors (SSRIs) [5, 6] and the serotonin noradrenaline reuptake inhibitor venlafaxine [6], while benzodiazepines may also be effective both in panic disorder and acute panic attacks [7]. However, overall rates of treatment efficacy and duration of illness have not improved since the previous generation of treatments (tricyclic antidepressants) [8, 9, 10]. Therefore, there is an unmet need for developing better therapeutics for the treatment of panic disorders.

Amiloride is a potassium-sparing diuretic currently approved by the Food and Drugs Administration (FDA) as an anti-hypertensive agent [11]. Amiloride was also shown to reduce anxiety symptoms in pre-clinical models by inhibiting acid-sensing ion channels (ASIC) channels in the brain [12, 13]. Amiloride is commercially available only as a tablet formulation for oral administration with an onset time of 2 hours and peak plasma levels reaching between 3 to 4 hours. For the treatment of panic attacks, rapid absorption of amiloride leading to a rapid onset of action, preferably within a few minutes, is highly desirable. Therefore, an intranasal administration route can be utilized to allow rapid absorption of the drug into the systemic circulation. Furthermore, this route can provide additional advantages, including rapid and extensive absorption, the ability to bypass the blood-brain barrier (BBB), and increased patient adherence [14, 15]. As a first step towards the clinical development of intranasal amiloride, we developed and characterized the formulation according to FDA guidance on intranasal products [16, 17].

It is important to characterize the pharmacokinetics (PK) of intranasal amiloride for a successful clinical translation to treat anxiety and panic disorders. The knowledge of PK is important because: 1) it provides the quantitative basis for developing a safe and effective dosage regimen, 2) it accounts for the biological barriers involved in the delivery of amiloride by the intranasal route, and 3) it provides a framework to evaluate the dose-response relationships between amiloride dose and its ability to reduce panic attacks. In this research project, we utilized a mathematical physiology-based pharmacokinetic (PBPK) modeling approach to predict amiloride plasma and brain PK after intranasal administration in the virtual human population [18]. While the PK of amiloride after oral inhalation using a nebulizer for the treatment of cystic fibrosis is known [19], this is the first report of a nasal PBPK model of amiloride that can predict its PK in human plasma, brain, and CSF after intranasal administration. PBPK modeling due to its mechanistic nature has been widely used in clinical translation of various drugs that are delivered as inhalation and nasal formulations [20, 21]. The oral PBPK model for amiloride was used as a base model for the nasal PBPK model and was verified for simulation accuracy using data obtained from 5 clinical studies. The present data will inform future clinical PK and efficacy studies and pave the way for the successful clinical translation of intranasal amiloride.

Materials and methods

Model parameters

The physicochemical and absorption, distribution, metabolism, and elimination

Table 1. Amiloride parameters used for PBPK model development.

Parameter (units)	Definition	Reported value	Optimized value	Ref.
log P	Lipophilicity	–0.49	–0.43	[22]
Unbound protein fraction (%)	N/A	60		[3]
Molecular weight (g/mol)	N/A	229.63		[3]
Compound type/pKa	Dissociation constant	Alkaline/ 8.70		[23]
Solubility at pH 7.4 (mg/mL)	N/A	5.2		[23]
Renal clearance (L/h)	N/A	25.0		[23]
P_{eff} ($\times 10^{-4}$ cm/s)	Effective permeability of amiloride across gastrointestinal epithelium	1.6		[24]
P_{PCSF} ($\times 10^{-4}$ cm/s)	Permeability amiloride across brain plasma to CSF	0.028		[25]
P_{ICSF} ($\times 10^{-4}$ cm/s)	Permeability amiloride across brain intracellular region to CSF	0.028		[25]
V_N (cm^3)	Volume of the nasal cavity	25		[26]
V_{SC} (cm^3)	Volume of blood compartment	420		[25]
V_{GI} (cm^3)		720		[25]
V_{RES} (cm^3)		1,210		[25]
V_B (cm^3)		1,440		[25]
V_{CSF} (cm^3)		140		[25]
V_P (cm^3)	in brain	32		[25]
SA_{NE} (cm^2/cm^3)	Surface area of the non-olfactory epithelium per unit volume of the nasal cavity	6.3		[26]
SA_{OE} (cm^2/cm^3)	Surface area of the olfactory epithelium per unit volume of the nasal cavity	0.51		[26]
SA_{GI} (cm^2/cm^3)	Surface area of the gastrointestinal tract per unit volume of the gastrointestinal tract	444		[27]
SA_{RES} (cm^2/cm^3)	Surface area of the respiratory tract per unit volume of the respiratory tract	578		[28]
SA_{PCSF} (cm^2/cm^3)	Surface area of CSF interfacing brain plasma per unit volume of the brain	180		[25]
SA_{ICSF} (cm^2/cm^3)	Surface area of CSF interfacing intracellular region of brain per unit volume of the brain	6.25		[25]

(ADME) properties of amiloride were obtained from literature sources and are reported in Table 1.

PBPK model development workflow

We first developed an oral PBPK model of amiloride and optimized it using amiloride concentration vs. time data after single- and multiple-dose administration from 5 clinical studies that reported PK of amiloride in humans [19, 29, 30, 31, 32]. We compared the distribution of the observed plasma concentration to the predicted plasma concentration of amiloride for a virtual population with demographic characteristics representative of all 5 studies. The finalized oral amiloride model served as the basis for developing the nasal PBPK model. In the nasal model, we sustained the physicochemical and drug-specific ADME parameters of amiloride and added nasal compartment using MoBi (Version 9.1 Build 2, Open Systems Pharmacology Suite, open-systems-pharmacology.org). The structure of the nasal PBPK model is provided in Figure 1. We performed simulations with virtual populations representing healthy human subjects to predict amiloride PK after intranasal administration.

Clinical data and software used

To provide the concentration vs. time data for the oral amiloride PBPK model development, we selected a total of 5 clinical studies. Four studies were based on a single-dose administration [19, 29, 31, 32], and 1 study used multiple-dose administration [30]. Multiple-dose administration data will help show that our model accurately predicts amiloride steady-state PK. We used the software Plot Digitizer (version 2.6.8) to extract the concentration vs. time data. The study details, including dose information, demographics, and analytical method used, are provided as Supplemental material S2 Table. The data files with plasma concentra-

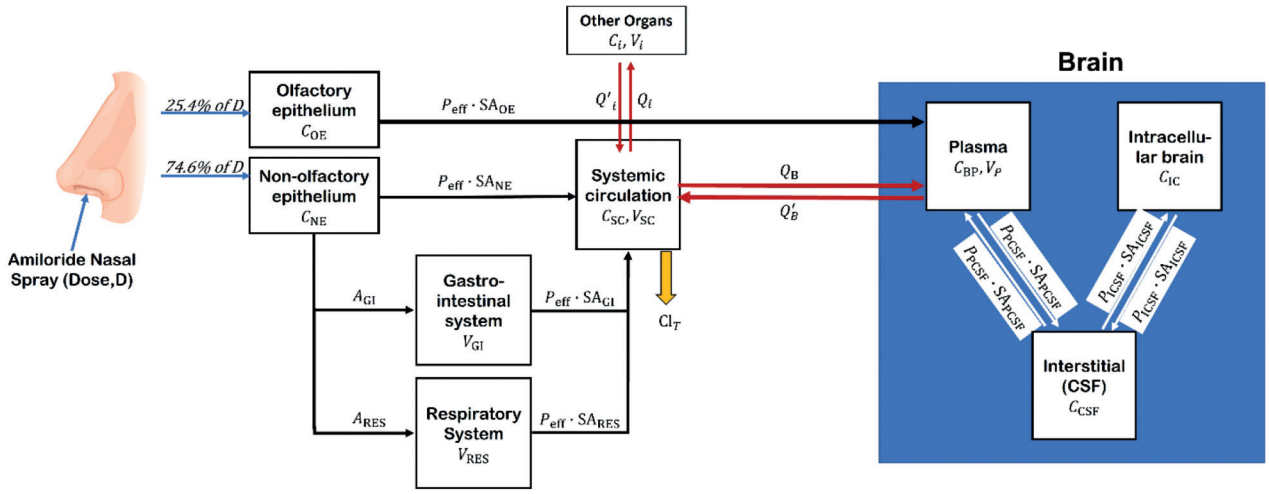

Figure 1. Schematic representation of nasal physiologically-based pharmacokinetic (PBPK) model of amiloride. C_{OE} = drug concentration in the olfactory epithelium; C_{NE} = drug concentration in the non-olfactory epithelium; A_{RES} = amount of drug entering the lungs; A_{GI} = amount of drug entering the gastrointestinal compartment; C_{IC} = concentration of drug in brain intracellular region; C_{CSF} = concentration of drug in CSF; C_{BP} = concentration of drug in brain plasma; C_i = concentration of drug in organ i. SA_{OE} = surface area of the olfactory epithelium of the nose; SA_{NE} = surface area the non-olfactory epithelium of the nose; SA_{GI} = surface area of the gastrointestinal tract; SA_{RES} = surface area of the respiratory tract; SA_{PCSF} = surface area of CSF interfacing with plasma; SA_{ICSF} = surface area of CSF interfacing the intracellular region of the brain; P_{eff} = effective permeability of amiloride across the gastrointestinal epithelium; P_{PCSF} = permeability of amiloride across brain plasma to CSF; P_{ICSF} = permeability of amiloride across the brain intracellular region to CSF; Q_B = blood flow rate to the brain; Q'_B = blood flow rate from the brain; Q_i = blood flow rate to organ i; Q'_i = blood flow rate from organ i . The volume (V), permeability (P), and surface area (SA) values are provided in Table 1. The values of blood flow rates are provided in Supplemental material (S1 Data).

tion vs. time profiles of all 5 studies are provided in Supplemental material S3 Data File.

We used PK Sim and MoBi (Version 9.1 Build 2, Open Systems Pharmacology Suite, open-systems-pharmacology.org) for model development and simulation. We used GraphPad Prism (Version 9, GraphPad LLC, San Diego, CA, USA) for data visualization.

Oral amiloride PBPK model development

We developed a standard whole-body PBPK model for the amiloride using PK-Sim, Version 9.1.-Build 2 (Open Systems Pharmacology Suite, http://www.open-systems-pharmacology.com). The initial base model was built using the amiloride human model after oral administration due to the availability of clinical PK data for verifying the model. The tissue or plasma partition coefficients were calculated using the PK-Sim standard model.

The cellular permeabilities for the barriers between interstitial space and intracellular space for amiloride were calculated from the physicochemical properties using PK Sim standard method. This method involves the calculation of permeability surface-area products of each organ. For the oral amiloride PBPK model, the oral formulation function was assumed to be dissolved. Amiloride is not metabolized by the liver and is excreted unchanged by the kidneys [22]. Therefore, renal excretion was considered as the only elimination mechanism for amiloride after systemic absorption. The total renal clearance value of amiloride was obtained from the literature [23]. We also compared the PK parameters $AUC_{0-\infty}$ and C_{max} of observed and simulated amiloride concentrations. To evaluate the model performance, we simulated concentration vs. time data in a virtual population with demographics (age and body weight) representative of all 5 clinical PK studies. The model's prediction accuracy was established by a visual prediction check. We considered the model final if the geometric mean ± SD of the simulated data captured > 80% of the observed data within the 90% prediction interval of the amiloride concentrations vs. time curve. For PK parameters, the model acceptance criteria within 0.5- to 2-fold was applied [33]. We optimized the lipophilicity

parameter using the parameter identification toolkit available in PK Sim.

Nasal PBPK model development

The oral amiloride PBPK model was exported into MoBi, where a new compartment reflecting the nasal cavity was added. The nasal compartment was modeled using 4 default sub-compartments: blood, plasma, interstitial fluid, and intracellular compartments [29]. These sub-compartments were linked to the entire PBPK model through arterial and venous blood compartments. The pathways for the absorption of amiloride after intranasal administration in the model included: nose to the brain via olfactory epithelium and trigeminal pathway, nose to the systemic circulation via nasal epithelium, lungs to the systemic circulation via respiratory epithelium, and gastrointestinal tract to systemic circulation due to swallowing of the drug. The volume of the nasal cavity was assigned as 25 cm^3 based on reported typical human nasal cavity volume [34]. The total amiloride dose administered was partitioned between the 4 pathways based on the liquid spray nasal deposition studies in humans [35]. We partitioned the total dose administered as 25.4% for the direct nose to brain pathway, 60.4% for the nose to systemic circulation pathway, 0.1% for the nose to lungs pathway, and 14.1% for the nose to gastrointestinal pathway based on published literature on nasal spray absorption patterns [35].

The absorption rate constants of amiloride transport from nose to brain (K_{NB}) and nose to the systemic circulation (K_{NS}) were calculated by multiplying the effective permeability (P_{eff}) of the drug with the surface area (SA_X) of each absorption site [26]. The P_{eff} value of amiloride was obtained as human intestinal permeability reported by Dahlgren et al. [24]. The absorption rate constants of amiloride for lungs to systemic circulation and stomach to systemic circulation were obtained from data published by Vulović et al. [23] and Dahlgren et al. [24], respectively. The differential equations used to model amiloride delivery to the brain following absorption through various pathways after nasal administration are provided in Supplemental material S4 Equations.

Simulations of amiloride PK after intranasal administration at various doses

The nasal amiloride PBPK model in MoBi was exported to PK Sim for population analyses. We created a virtual healthy adult population (N = 100) using PK Sim's default healthy adult individual parameters. We simulated amiloride PK in this virtual population at various doses between 5 and 75 mg. For simplicity, we considered the dosage form for intranasal administration as a nasal spray solution. We calculated the PK of amiloride in plasma, brain tissue, and cerebrospinal fluid (CSF) in the virtual population at different doses. The brain was modeled using the following 4 default sub-compartments: blood, plasma, interstitial fluid (representing the CSF) [36], and intracellular compartments [29]. These sub-compartments were linked to the entire PBPK model through arterial and venous blood compartments. We also simulated amiloride PK in brain sub-compartments after oral administration and compared them with simulations after intranasal administration at the same doses.

Results

Oral PBPK model

Optimized oral PBPK model predictions vs. observed data from the 4 single-dose oral datasets showed good agreement, with over 80% of the observed data within the 90% prediction interval of the simulated population concentrations (Figure 2). The doses in 4 studies varied between 2.5 mg to 10 mg and involved both liquid and tablet formulations (Supplemental material S2 Table). The optimized oral PBPK model also accurately predicted the steady-state (6-day multiple-dosing) PK of amiloride after multiple-dose administration. The model predictions vs. observed data from the multiple-dose oral dataset showed good agreement, with the majority of the observed data falling within the 90% prediction interval of the simulated population concentrations (Figure 3). To further evaluate the model's prediction accuracy, we compared the PK parameters t_{max}, $AUC_{0-\infty}$, and C_{max}. The t_{max}, $AUC_{0-\infty}$, and C_{max} values from simulated data were within the

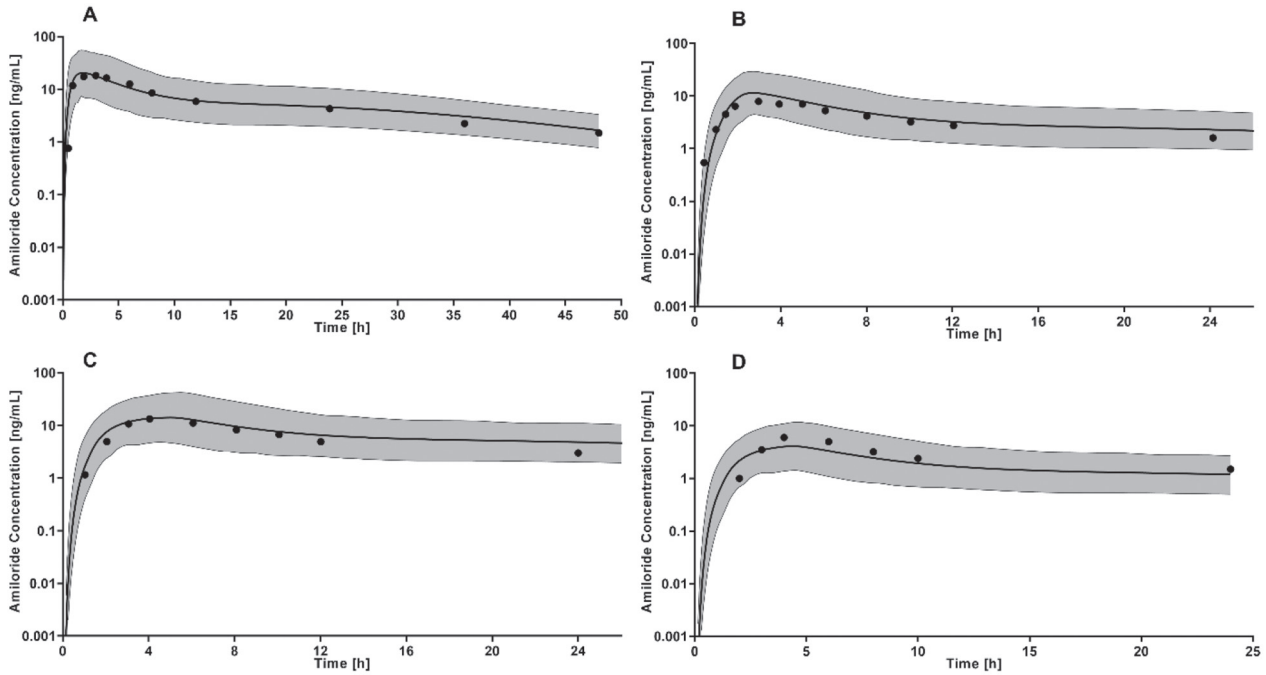

Figure 2. Observed and physiologically based pharmacokinetic (PBPK) model-simulated concentrations of amiloride in plasma after single-dose oral administration in the human population. The black circle symbols represent the mean amiloride concentration of the observed data from the following clinical studies: A: A single 10-mg oral dose of amiloride as 10-mL solution in 19 patients with mild-to-moderate cystic fibrosis [19]; B: A single 5-mg oral dose of amiloride as capsules in 12 healthy subjects [32]; C: a single 10-mg oral dose of amiloride as tablets in 12 healthy subjects [29]; and D: a single 2.5-mg amiloride oral dose as a capsule in 6 healthy subjects [31]. The solid lines represent geometric means of the amiloride plasma concentrations from the PBPK model. The shaded region represents the 90% prediction interval for the simulated amiloride concentrations.

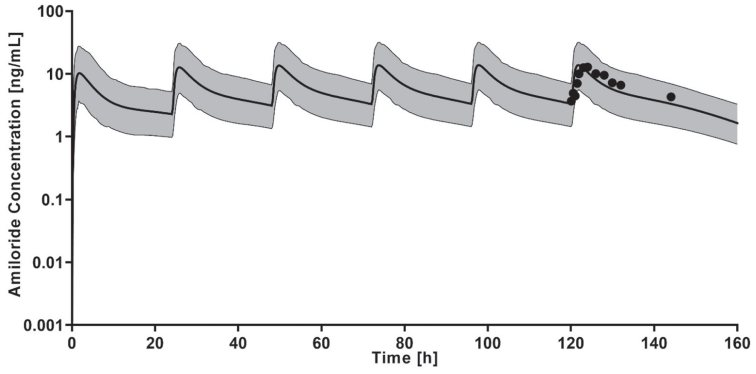

Figure 3. Observed and physiologically based pharmacokinetic (PBPK) model-simulated concentrations of amiloride in plasma after multiple-dose oral administration in the human population. The black circle symbols represent the mean amiloride concentration of the observed data from the clinical study where 8 participants received 5 mg amiloride as tablets for 6 days, and the blood samples were collected on the seventh day [30]. The solid line represents the geometric mean of the amiloride plasma concentrations from the PBPK model. The shaded region represents the 90% prediction interval for the simulated amiloride concentrations.

predetermined 0.5- to 2-fold acceptance criteria of the PK parameter observed in all 5 clinical studies (Table 2). These data suggest that our oral PBPK model is robust and has good prediction accuracy with single- and multiple-dose and different dosage forms of amiloride.

Intranasal PBPK model

The optimized oral PBPK model was directly imported into MoBi without any further modifications, and the nasal compartment was successfully added. The concentration vs. time curve for amiloride in plasma, brain tissue, and CSF after intranasal administration showed a biphasic response with a rapid increase in brain concentrations, followed by a decline, and then the concentration increasing slowly (Figure 4). The first rapid spike (0.1 hours) in brain and CSF concentrations can be attributed to the rapid absorption of amiloride through the olfactory epithelium, and the second more gradual increase in brain and CSF concentrations are due to a combination of the absorption via nasal epithelium, respiratory

Table 2. Observed and simulated PK parameters from oral amiloride PBPK model.

	Observed data			Simulation data			Mean ratio of simulated/observed		
	$AUC_{0-\infty}$ (ng×h/mL)	C_{max} (ng/mL)	t_{max} (h)	$AUC_{0-\infty}$ (ng×h/mL)	C_{max} (ng/mL)	t_{max} (h)	$AUC_{0-\infty}$	C_{max}	t_{max}
Jones et al. [19]	275 ± 115	20.6 ± 10	3.2	298.2	20.5	1.8	1.0	0.9	0.5
Brooks et al. [29]	149.9 ± 62.8	13.9 ± 5.8	4	298.2	20.5	5	1.9	1.4	1.2
Flouvat et al. [32]	115 ± 16.9	8.3 ± 1.6	3	150	10.6	2.75	1.3	1.2	0.9
Sabanathan et al. [31]	89.7 ± 6.8	5.9 ± 0.8	4	98.1	5.1	4.5	1.0	0.8	1.1
Somogyi et al. [30]	174.3 ± 53.6	14.3 ± 3.1	3	217.2	13.8	1.8	1.2	0.9	0.6

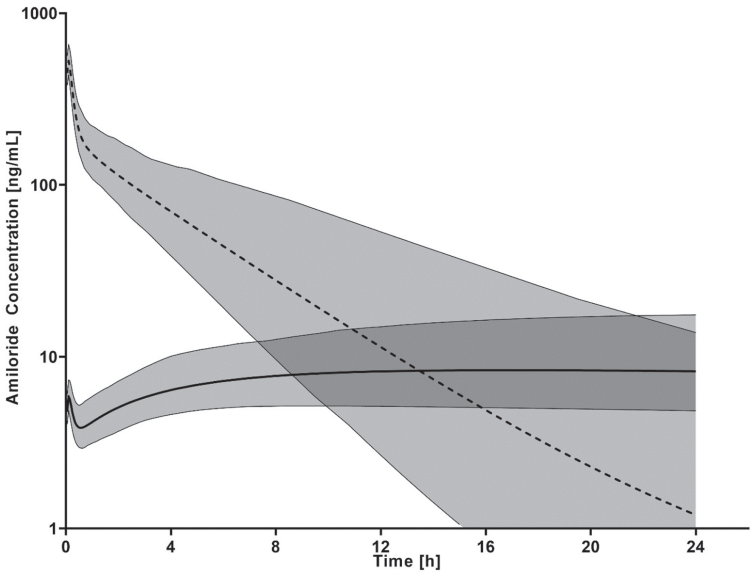

Figure 4. The physiologically based pharmacokinetic model concentration-time model predictions of amiloride in brain tissue and CSF after 25-mg dose of intranasal amiloride. The solid line represents the geometric mean of amiloride concentrations in brain tissue, and the dashed line represents the geometric mean of the amiloride concentrations in CSF from the nasal PBPK model. The shaded region represents the 90% prediction interval for the simulated amiloride concentrations.

epithelium, and gastrointestinal epithelium to the systemic circulation.

As expected, the PK parameters $AUC_{0-\infty}$ and C_{max} of amiloride in plasma, brain, and CSF showed a dose-dependent increase (Table 3). The t_{max} of amiloride in plasma and brain tissues was 0.15 hours and 0.1 hours, respectively. The shorter t_{max} of amiloride in brain tissues suggests a direct nose-to-brain transport of amiloride after intranasal administration. The C_{max} of amiloride in CSF is much higher than the C_{max} in brain tissue, which may be due to the unusual solubility behavior of amiloride, where even though it has low lipophilicity (Log P = -0.43) it is sparingly soluble in water (~ 1 mg/mL). The relative bioavailability (F) of amiloride nasal spray with reference to the oral tablet was 4.18, indicating an overall increase in systemic absorption of amiloride after nasal administration. Furthermore, the simulations after oral administration at the same dose (75 mg) as that of intranasal administration showed that C_{max} (0.11 µg/mL) is significantly smaller, and t_{max} (1.65 hours) is significantly longer in CSF when compared to intranasal administration.

Discussion

We developed a nasal PBPK model of amiloride from an optimized oral PBPK model to predict PK in the brain and CSF after intranasal administration. ••• **The ratio of simulated vs. observed values of the PK**

Table 3. Simulated plasma, brain, and CSF PK parameters of intranasal amiloride.

	Plasma PK parameters			Brain tissue PK parameters			CSF PK parameters		
Dose (mg)	t_{max} (h)	C_{max} (µg/mL)	$AUC_{0-\infty}$ (µg×h/mL)	t_{max} (h)	C_{max} (µg/mL)	$AUC_{0-\infty}$ (µg×h/mL)	t_{max} (h)	C_{max} (µg/mL)	$AUC_{0-\infty}$ (µg×h/mL)
1	0.15	0.05	0.12	0.1	0.003	0.1	0.1	0.05	0.088
5	0.15	0.29	0.62	0.1	0.0016	0.5	0.1	0.26	0.044
25	0.15	1.45	3.12	0.1	0.08	2.53	0.1	1.31	2.2
50	0.15	2.9	6.24	0.1	0.016	5.08	0.1	2.63	4.4
75	0.15	4.35	9.36	0.1	0.025	7.62	0.1	3.95	6.6

parameters t_{max}, $AUC_{0-\infty}$, and C_{max} within the 0.5- to 2-fold parameter for our oral PBPK model [**••• Sentence incomplete**]. To our knowledge, this is the first report of the nasal PBPK model of amiloride. Our model has high clinical significance as amiloride can be delivered intranasally to treat panic attacks rapidly in anxiety disorder patients. The PBPK model developed by us in this research has been previously utilized by other investigators to characterize the plasma and central nervous system exposure of fluconazole in adult and pediatric patients [36]. Furthermore, the structure of the intranasal PBPK model that we developed was also previously utilized by Kadakia et al. [26] to predict the transport of drug to the brain after intranasal administration.

The only other administration route where amiloride was investigated in clinical studies apart from the oral route is the oral inhalational route of administration. Jones et al. [19] reported a clinical PK study involving the delivery of amiloride via oral inhalational route using a nebulizer in cystic fibrosis patients. Because the lung deposition of a drug administered as a nasal spray is less than 0.1% [35], we did not use the oral inhalational PK data of amiloride from the published clinical studies to verify our nasal PBPK of amiloride. As expected, the PK of amiloride after oral inhalation administration were quite different from the simulated PK of amiloride after intranasal administration. For example, the plasma t_{max} of amiloride after intranasal administration was 0.15 hours, which was significantly lower than the t_{max} after oral inhalational administration of 0.5 hours. Interestingly, both $AUC_{0-\infty}$ and C_{max} (14.4 ng×h/mL, and 1.37 ng/mL) of amiloride after oral inhalational administration at 4.5-mg dose [19] were significantly lower compared to the $AUC_{0-\infty}$ and C_{max} after intranasal administration (624.52 ng×h/mL, and 290.24 ng/mL, respectively) at 5-mg dose (Table 3). Furthermore, the absorption rate (K_a) calculated using C_{max} to $AUC_{0-\infty}$ ratio of amiloride is 0.095 h^{-1} after inhalation administration, which is significantly lower than the K_a of 0.465 h^{-1} intranasal administration. The increase in bioavailability of amiloride after intranasal administration, when compared with the oral inhalational route, needs further exploration.

It is well established that ASICs are enriched in human neurons and are distributed widely in the central nervous system [13, 37]. Accumulating evidence has shown that ASICs activation is implicated in several physiological processes, including fear behaviors [38], nociception [39], and brain ischemia [40]. The studies on the membrane topology of ASICs have confirmed that ASICs are predominantly present as extracellular domains on cells and are activated by changes in the extracellular environment [41, 42]. Therefore, the concentration of amiloride in brain extracellular fluid, which is mainly comprised of CSF, is the major determinant of amiloride's anti-anxiety efficacy rather than the brain tissue concentrations. Consequently, to reduce the onset of panic attacks, it is imperative that amiloride rapidly reach high concentrations in CSF after intranasal administration. Leng et al. [13] reported that the IC_{50} value for amiloride's ASICs inhibition efficacy is 3.17 μg/mL from in vitro experiments on isolated human cortical neurons. The nasal PBPK model of amiloride predicted that a C_{max} of 3.17 μg/mL can be achieved after administering a dose of 60.1 mg in a virtual human population (Table 3). This indicates that the intranasal dose of 75 mg is ideal to achieve optimal ASIC inhibition activity in the human brain as this dose will result in concentrations that are significantly higher than 3.17 μg/mL. The simulations of amiloride PK in CSF after oral administration showed at 75-mg dose that the C_{max} is significantly lower (0.11 μg/mL) than the target C_{max} (3.17 μg/mL), and the intranasal route of administration is the preferred route to maximize the delivery of amiloride to the brain. This information is valuable for successfully translating intranasal amiloride as a treatment option for reducing panic attacks. Furthermore, the optimal amiloride dose required to achieve maximal ASIC inhibition activity will help develop an intranasal formulation. However, our nasal PBPK model's simulations need to be verified with data from a prospective clinical trial in healthy subjects using intranasal amiloride. To that end, we obtained an investigator-initiated new drug application approval from the FDA to evaluate the PK of intranasal amiloride in healthy human subjects, and we are currently enrolling participants for the study [43].

Some limitations of this model need to be considered. First, the nasal amiloride PBPK model requires verification with clinical data to confidently make clinical decisions based on the model predictions. However, this first report of an oral PBPK model of amiloride verified data from 5 clinical studies and added a nasal cavity compartment to predict amiloride PK after intranasal administration. Second, the permeability coefficient (P_{eff}) value used to calculate the absorption rate constants of amiloride across the olfactory epithelium and nasal epithelium was obtained from human gastrointestinal epithelium experiments. We assumed that the difference in permeability of amiloride across olfactory, nasal, and gastrointestinal tissues is negligible as amiloride follows a passive diffusion pathway for transport across the membranes. However, to improve the accuracy of nasal model prediction, the permeability of amiloride across olfactory and nasal epithelium needs to be calculated by ex vivo experiments using isolated tissues.

Conclusion

In conclusion, a nasal PBPK model of amiloride was developed from an oral PBPK optimized model using data from 5 clinical studies. Using the nasal PBPK model of amiloride, we successfully simulated the PK of amiloride in plasma and CSF after intranasal administration of amiloride at various doses. However, our simulations need to be validated and verified using clinical or experimental data. The PK parameters of amiloride in CSF were correlated with amiloride's ASIC inhibition activity data obtained from in vitro experiments, and an ideal dose for maximal therapeutic efficacy was identified. However, the ideal dose needs to be validated using clinical pharmacodynamic data. The nasal PBPK model of amiloride could be valuable for further clinical translation of intranasal amiloride as a therapeutic product to treat anxiety disorders. Future developments include examining clinical PK of intranasal amiloride prospectively in healthy human subjects and developing optimal intranasal amiloride formulation to achieve maximal brain exposure.

Supplemental material

S1 Data: Datafile containing complete details of the physiological parameters including organ and tissue sizes, blood flow rates to each organ and tissues, and tissue to plasma partition coefficients for amiloride oral PBPK model.

S2 Table: Table with details of clinical studies used for the verification of oral PBPK model.

S3 Data: Datafiles of observed data with mean amiloride plasma concentrations extracted from 5 clinical studies.

S4 Equations: List of differential equations used for the development of the amiloride intranasal PBPK model.

Authors' contributions

Conceptualization: VY, MB, SD, JS, and MA; methodology: VY, MA; software: VY, MB, PD; formal analysis: VY, MA, PD; writing – original draft preparation: MA, VY; writing – review & editing: MA, VY, SD, JS, MB, PD.; funding acquisition, MB, SD.

Funding

The project was supported by the CAMH Foundation Discovery grant to MB.

Conflict of interest

The authors declare no conflict of interest.

References

[1] *Bandelow B, Michaelis S*. Epidemiology of anxiety disorders in the 21st century. Dialogues Clin Neurosci. 2015; *17:* 327-335.

[2] *Sylvester CM, Hudziak JJ, Gaffrey MS, Barch DM, Luby JL*. Stimulus-Driven Attention, Threat Bias, and Sad Bias in Youth with a History of an Anxiety Disorder or Depression. J Abnorm Child Psychol. 2016; *44:* 219-231.

[3] *DuPont RL, Rice DP, Miller LS, Shiraki SS, Rowland CR, Harwood HJ*. Economic costs of anxiety disorders. Anxiety. 1996; *2:* 167-172.

[4] *Association A. P.* [**●●● Please check author name**] Diagnostic and Statistical Manual of Mental Disorders, 5th Edition: DSM-5; 2013.

[5] *Baldwin DS, Anderson IM, Nutt DJ, Bandelow B, Bond A, Davidson JR, den Boer JA, Fineberg NA, Knapp M, Scott J, Wittchen HU*; *British Associa-*

tion for Psychopharmacology. Evidence-based guidelines for the pharmacological treatment of anxiety disorders: recommendations from the British Association for Psychopharmacology. J Psychopharmacol. 2005; *19:* 567-596.

[6] *Katzman MA, Bleau P, Blier P, Chokka P, Kjernisted K, Van Ameringen M, Antony MM, Bouchard S, Brunet A, Flament M, Grigoriadis S, Mendlowitz S, O'Connor K, Rabheru K, Richter PM, Robichaud M, Walker JR*; *Canadian Anxiety Guidelines Initiative Group on behalf of the Anxiety Disorders Association of Canada/Association Canadienne des troubles anxieux and McGill University*. Canadian clinical practice guidelines for the management of anxiety, posttraumatic stress and obsessive-compulsive disorders. BMC Psychiatry. 2014; *14* (*Suppl 1*)*:* S1.

[7] *Ziffra M*. Panic disorder: A review of treatment options. Ann Clin Psychiatry. 2021; *33:* 124-133.

[8] *Pollack MH, Otto MW, Kaspi SP, Hammerness PG, Rosenbaum JF*. Cognitive behavior therapy for treatment-refractory panic disorder. J Clin Psychiatry. 1994; *55:* 200-205.

[9] *Katon WJ*. Clinical practice. Panic disorder. N Engl J Med. 2006; *354:* 2360-2367.

[10] *Kessler RC, Chiu WT, Jin R, Ruscio AM, Shear K, Walters EE*. The epidemiology of panic attacks, panic disorder, and agoraphobia in the National Comorbidity Survey Replication. Arch Gen Psychiatry. 2006; *63:* 415-424.

[11] *Pharmaceutical P*. [●●● **Please check author name**] Amiloride Hydrochloride, Drug Label Information. https://dailymed.nlm.nih.gov/dailymed/drugInfo.cfm?setid=e0cc2d44-436a-47e8-a890-589882fff4c4. 2018.

[12] *Battaglia M, Rossignol O, Bachand K, D'Amato FR, De Koninck Y*. Amiloride modulation of carbon dioxide hypersensitivity and thermal nociceptive hypersensitivity induced by interference with early maternal environment. J Psychopharmacol. 2019; *33:* 101-108.

[13] *Leng TD, Si HF, Li J, Yang T, Zhu M, Wang B, Simon RP, Xiong ZG*. Amiloride Analogs as ASIC1a Inhibitors. CNS Neurosci Ther. 2016; *22:* 468-476.

[14] *Chapman CD, Frey WH II, Craft S, Danielyan L, Hallschmid M, Schiöth HB, Benedict C*. Intranasal treatment of central nervous system dysfunction in humans. Pharm Res. 2013; *30:* 2475-2484.

[15] *Djupesland PG, Messina JC, Mahmoud RA*. The nasal approach to delivering treatment for brain diseases: an anatomic, physiologic, and delivery technology overview. Ther Deliv. 2014; *5:* 709-733.

[16] *Yellepeddi V, Sayre C, Burrows A, Watt K, Davies S, Strauss J, Battaglia M*. Stability of extemporaneously compounded amiloride nasal spray. PLoS One. 2020; *15:* e0232435.

[17] *Industry Guidance on Inhalational and Nasal Products*. FDA. https://www.fda.gov/media/70857/download.

[18] *Dogra P, Butner JD, Ruiz Ramírez J, Chuang YL, Noureddine A, Jeffrey Brinker C, Cristini V, Wang Z*. A mathematical model to predict nanomedicine pharmacokinetics and tumor delivery. Comput Struct Biotechnol J. 2020; *18:* 518-531.

[19] *Jones KM, Liao E, Hohneker K, Turpin S, Henry MM, Selinger K, Hsyu PH, Boucher RC, Knowles MR, Dukes GE*. Pharmacokinetics of amiloride after inhalation and oral administration in adolescents and adults with cystic fibrosis. Pharmacotherapy. 1997; *17:* 263-270.

[20] *Tang C, Ou-Yang CX, Chen WJ, Zou C, Huang J, Cui C, Yang S, Guo C, Yang XY, Lin Y, Pei Q, Yang GP*. Prediction of pharmacokinetic parameters of inhaled indacaterol formulation in healthy volunteers using physiologically-based pharmacokinetic (PBPK) model. Eur J Pharm Sci. 2022; *168:* 106055.

[21] *Khalid S, Rasool MF, Imran I, Majeed A, Saeed H, Rehman AU, Ashraf W, Ahmad T, Bin Jardan YA, Alqahtani F*. A Physiologically Based Pharmacokinetic Model for Predicting Diazepam Pharmacokinetics after Intravenous, Oral, Intranasal, and Rectal Applications. Pharmaceutics. 2021; *13:* 1480.

[22] Clinical Pharmacology. Amiloride Human Prescription Drug Label. https://dailymed.nlm.nih.gov/dailymed/drugInfo.cfm?setid=dc7aef5e-9585-45b9-b317-4af570202ef5. Accessed on March 19, 2021.

[23] *Vulović A, Šušteršič T, Cvijić S, Ibrić S, Filipović N*. Coupled in silico platform: Computational fluid dynamics (CFD) and physiologically-based pharmacokinetic (PBPK) modelling. Eur J Pharm Sci. 2018; *113:* 171-184.

[24] *Dahlgren D, Roos C, Sjögren E, Lennernäs H*. Direct In Vivo Human Intestinal Permeability (Peff) Determined with Different Clinical Perfusion and Intubation Methods. J Pharm Sci. 2015; *104:* 2702-2726.

[25] *Bayer Technology Services*. Computational systems biology software suite. PKSim® and MOBI® manual. Version 7.0.0, SB Suite http://www.systems-biolo gy.com/produ cts/pk-sim.html. Accessed March 10, 2021.

[26] *Kadakia E, Bottino D, Amiji M*. Mathematical Modeling and Simulation to Investigate the CNS Transport Characteristics of Nanoemulsion-Based Drug Delivery Following Intranasal Administration. Pharm Res. 2019; *36:* 75.

[27] *Helander HF, Fändriks L*. Surface area of the digestive tract - revisited. Scand J Gastroenterol. 2014; *49:* 681-689.

[28] *Fröhlich E, Mercuri A, Wu S, Salar-Behzadi S*. Measurements of Deposition, Lung Surface Area and Lung Fluid for Simulation of Inhaled Compounds. Front Pharmacol. 2016; *7:* 181.

[29] *Brooks SG, Christie RB, Roche J, Fairhead AP, Muirhead D, Townsend HA, Shaw HL*. Pharmacokinetics of an oral frusemide/amiloride combination tablet. Curr Med Res Opin. 1984; *9:* 141-146.

[30] *Somogyi A, Hewson D, Muirhead M, Bochner F*. Amiloride disposition in geriatric patients: importance of renal function. Br J Clin Pharmacol. 1990; *29:* 1-8.

[31] *Sabanathan K, Castleden CM, Adam HK, Ryan J, Fitzsimons TJ*. A comparative study of the pharmacokinetics and pharmacodynamics of atenolol, hydrochlorothiazide and amiloride in normal young and elderly subjects and elderly hypertensive patients. Eur J Clin Pharmacol. 1987; *32:* 53-60.

[32] *Flouvat B, Roux A, Leneveu A, Prinseau J, Alexandre JA*. Combination of long-acting furosemide and instant-acting amiloride: pharmacokinetics and pharmacodynamics in human subjects. Fundam Clin Pharmacol. 1991; *5:* 741-752.

[33] *Jo H, Pilla Reddy V, Parkinson J, Boulton DW, Tang W*. Model-Informed Pediatric Dose Selection for Dapagliflozin by Incorporating Developmental

Changes. CPT Pharmacometrics Syst Pharmacol. 2021; *10:* 108-118.

[34] *Liu Y, Johnson MR, Matida EA, Kherani S, Marsan J*. Creation of a standardized geometry of the human nasal cavity. J Appl Physiol (1985). 2009; *106:* 784-795.

[35] *Djupesland PG, Skretting A*. Nasal deposition and clearance in man: comparison of a bidirectional powder device and a traditional liquid spray pump. J Aerosol Med Pulm Drug Deliv. 2012; *25:* 280-289.

[36] *Gerhart JG, Watt KM, Edginton A, Wade KC, Salerno SN, Benjamin DK Jr, Smith PB, Hornik CP, Cohen-Wolkowiez M, Duara S, Ross A, Shattuck K, Stewart DL, Neu N, Gonzalez D, Furda G, Benjamin D, Capparelli E, Kearns GL, Paul IM, et al*; *Best Pharmaceuticals for Children Act-Pediatric Trials Network Steering Committee*. Physiologically-Based Pharmacokinetic Modeling of Fluconazole Using Plasma and Cerebrospinal Fluid Samples From Preterm and Term Infants. CPT Pharmacometrics Syst Pharmacol. 2019; *8:* 500-510.

[37] *Li M, Inoue K, Branigan D, Kratzer E, Hansen JC, Chen JW, Simon RP, Xiong ZG*. Acid-sensing ion channels in acidosis-induced injury of human brain neurons. J Cereb Blood Flow Metab. 2010; *30:* 1247-1260.

[38] *Wemmie JA, Askwith CC, Lamani E, Cassell MD, Freeman JH Jr, Welsh MJ*. Acid-sensing ion channel 1 is localized in brain regions with high synaptic density and contributes to fear conditioning. J Neurosci. 2003; *23:* 5496-5502.

[39] *Wemmie JA, Taugher RJ, Kreple CJ*. Acid-sensing ion channels in pain and disease. Nat Rev Neurosci. 2013; *14:* 461-471.

[40] *Pignataro G, Cuomo O, Esposito E, Sirabella R, Di Renzo G, Annunziato L*. ASIC1a contributes to neuroprotection elicited by ischemic preconditioning and postconditioning. Int J Physiol Pathophysiol Pharmacol. 2011; *3:* 1-8.

[41] *Saugstad JA, Roberts JA, Dong J, Zeitouni S, Evans RJ*. Analysis of the membrane topology of the acid-sensing ion channel 2a. J Biol Chem. 2004; *279:* 55514-55519.

[42] *Sherwood TW, Frey EN, Askwith CC*. Structure and activity of the acid-sensing ion channels. Am J Physiol Cell Physiol. 2012; *303:* C699-C710.

[43] [**●●● Please include all authors**]. Pharmacokinetics of Amiloride Nasal Spray in Healthy Volunteers. https://clinicaltrials.gov/ct2/show/NCT04181008?term=yellepeddi&draw=2&rank=1.